UTCI-Fiala multi-node model of human heat transfer and temperature regulation

Dusan Fiala[1,2]✉, George Havenith[3], Peter Bröde[4], Bernhard Kampmann[5], Gerd Jendritzky[6]

[1] Ergonsim – Comfort Energy Efficiency, Stuttgart, Germany

[2] Institute of Building Technologies (IBBTE), University of Stuttgart, Stuttgart, Germany

[3] Environmental Ergonomics Research Centre, Loughborough University, UK

[4] Leibniz Research Centre for Working Environment and Human Factors (IfADo), Dortmund, Germany

[5] Bergische Universität Wuppertal, Division of Applied Physiology, Occupational Medicine and Infectiology, Department of Safety Engineering, Germany

[6] Meteorological Institute, Albert-Ludwigs-Universität Freiburg, Germany

✉ Corresponding author:

Dr. Dusan Fiala

ErgonSim – Comfort Energy Economy

Holderbuschweg 47

70563 Stuttgart

Germany

Phone +49 7202 40 90 65

Fax   +49 711 5042 1774

e-mail: dfiala@ergonsim.de

http://www.ergonsim.de

Abstract

The UTCI-Fiala mathematical model of human temperature regulation forms the basis of the new UTC Index. Following extensive validation tests, adaptations and extensions such as the inclusion of an adaptive clothing model, the model was used to predict human temperature and regulatory responses for combinations of the prevailing outdoor climate conditions. This paper provides an overview of the underlying algorithms and methods that constitute the multi-node dynamic UTCI-Fiala model of human thermal physiology and comfort. Treated topics include modelling heat and mass transfer within the body, numerical techniques, modelling environmental heat exchanges, thermoregulatory reactions of the central nervous system and perceptual responses. Other contributions of this special issue describe the validation of the UTCI-Fiala model against measured data and the development of the adaptive clothing model for outdoor climates.

Keywords

Introduction

One of the driving impulses for developing the *Universal Thermal Climate Index* (UTCI) has been the growing need from different disciplines for a physiological response-based assessment index that is valid across a broad spectrum of outdoor climate conditions including weather extremes. There has been a consensus among experts in the field that the new index should incorporate up-to-date knowledge in human thermal physiology and biophysics and take into account (i) the complete human heat budget and (ii) thermal physiological response of an average human subject. Considering the scientific advances in thermophysiological modelling of the past four decades, the COST Action 730 experts thus decided to develop UTCI based on the most advanced *multi-node* model(s) of human thermoregulation.

Mathematical modelling of human thermal regulation and comfort goes back some 70 years. Following diverse general human heat balance considerations (e.g. Burton 1937, Aschoff and Wever 1958, Fanger 1973) various two-node models of human thermoregulation emerged (e.g. Azer and Hsu 1977, Gagge et al. 1986). In the past forty years, also more complex, multi-segmental models (e.g. Stolwijk 1971, Wissler 1985, Huizenga et al. 2001, Tanabe et al. 2002, Fiala et al. 1999 - 2003) have been developed. Compared to two-node models, multi-segmental (here: multi-node) models simulate the human body in greater detail predicting both overall and local physiological responses. Human environmental heat losses are calculated taking into account characteristic inhomogeneities such as non-uniform skin temperatures, regulatory responses, clothing properties or environmental conditions. Heat dissipation within the body is predicted by explicit simulation of the individual human heat transfer components (including blood circulation) using thermal and physiological properties of the main tissue types and taking into consideration the specific role of extremities in human thermoregulation.

Following inter-comparisons within a suite of contemporary simulation models (subject to model availability), and extensive validation against human thermophysiological experimental observations, the Fiala model was selected to form the basis of the new Universal Thermal Climate Index (UTCI). In previous work, this model has found multiple applications e.g. in architecture and the built environment; automotive industry; clothing research, clinical and safety research, and in medical engineering (for a review see Fiala et al. 2010).

For use in conjunction with UTCI it was important to ensure, that the model is able to reproduce the human thermal behaviours of an average, unacclimatised subject in response to wide-ranging outdoor climate conditions. These are characterised by non-moderate ambient temperatures, elevated wind speeds, and solar radiation conditions. A description of the COST 730 validation and inter-model comparison exercise is provided by Psikuta et al. (2011), Bröde et al. (2011b), and Kampmann et al. (2010) in this special issue.

A special version of the Fiala model – the *UTCI-Fiala* model, was set up for purposes of the COST Action 730. In this version the original model was adapted and extended to predict human responses specifically to outdoor climate conditions. As UTCI is a direction-independent index, the original 19-compartment, 342-node model is configured as a symmetric 12-compartment, 187-node model whose left and right extremities and spatial body sectors are merged to lumped entities. The work also involved development and implementation of algorithms for calculating solar absorption rates at irradiated body parts for *unknown* body orientations based on Kubaha et al. (2004).

Another extension of the physiological model dealt with the development and implementation of an adaptive outdoor clothing model. This model takes into account behavioural adjustments of the clothing insulation with outdoor air temperature and considers the effect of wind, walking speed and clothing permeability on clothing's thermal and evaporative resistances as described by Havenith et al. (2011) in this special issue. Further modifications included the computation of local air velocities at body element levels from meteorological measurements of the wind speed and the reduction of shivering during physical exercise.

This article provides a general overview of the UTCI-Fiala multi-node model. The paper summarises the underlying algorithms that constitute the model based on material published by Fiala (1998) and Fiala et al. (1999-2003).

Body construction

The UTCI-Fiala model consists of 12 spherical or cylindrical body compartments: *head, face, neck, shoulders, thorax, abdomen, upper* and *lower arms, hands, upper* and *lower legs,* and *feet* (**Figure 1**). Body elements are built of annular concentric tissue layers (section A-A″ in **Figure 1**): *brain, lung, bones, muscles, viscera, fat,* and *skin* (Fiala et al. 1999) and subdivided into a total of 63 spatial sectors (**Table 1**). Skin is modelled as two layers (Weinbaum et al. 1984): cutaneous plexus, i.e. blood-perfused inner layer; and outer skin which contains sweat glands but no thermally significant blood vessels. This superficial skin layer also simulates the vapour barrier for moisture diffusion through the skin in the model.

(**Figure 1** about here)

The model represents an *average* person with a body surface area of 1.85 m², body weight of 73.4 kg, and body fat content of 14%. The overall physiological data of the computer humanoid replicates a reclining adult with a basal whole body metabolism of 87.1 W, basal evaporation rate

4

from the skin of 18 W, cardiac output of 4.9 L min⁻¹, skin blood flow of 0.4 L min⁻¹; and skin wettedness of 6 %;

(**Table 1** about here)

Heat transfer within the body

Bioheat transfer equation

The dynamic heat and mass transport within the body is modelled using the Bio-Heat Transfer Equation of Pennes (1948) formulated for polar and spherical coordinates (Fiala et al. 1999):

$$\rho c \frac{\partial T}{\partial t} = k \left(\frac{\partial^2 T}{\partial r^2} + \frac{\omega}{r} \frac{\partial T}{\partial r} \right) + \rho_{bl} w_{bl} c_{bl} \left(T_{bla} - T \right) + q_m$$

(1)

where, ρ [kg m⁻³] is tissue density, c [J kg⁻¹ K⁻¹] tissue heat capacitance, T [°C] tissue temperature, t [s] time, k [W m⁻¹ K⁻¹] tissue conductivity,, r [m] radius, ω is a geometry factor (ω=1 for polar co-ordinates, ω=2 for spheres), T_{bla} [°C] arterial blood temperature, ρ_{bl} [kg m⁻³] density of blood, w_{bl} [m³ s⁻¹ m⁻³] blood perfusion rate, c_{bl} [J kg⁻¹ K⁻¹] heat capacitance of blood, and q_m [W m⁻³]metabolism.

In the numerical model each tissue layer is discretized as one or more *tissue nodes* (see **Figure 1**, section A-A") summing up to 187 tissue nodes for the body as a whole. To minimize numerical error, tissue nodes are spaced unequally in radial direction with a denser spacing towards outer body regions where the steepest temperature gradients occur.

A finite-difference scheme is employed to discretize eq. (1) in the numerical model. The partial derivatives with radius are modelled using the *central difference method*. The partial derivative for temporal changes in tissue temperature is approximated using the *Crank-Nicholson* scheme ($\Omega_{CN} T_r$), which is constituted by averaging the explicit ($\Omega_{Ex} T_r$) and the implicit ($\Omega_{Im} T_r$) method defined for the current time-step (t) and the 'future' time-step (t+1), respectively:

$$\Omega_{CN} T_r^{(t)} = \frac{1}{2} \left(\Omega_{Ex} T_r^{(t)} + \Omega_{Im} T_r^{(t+1)} \right)$$

(2)

Applied to eq. (1) the explicit and the implicit expressions for node *r* yield:

$$\Omega_{Ex} T_r^{(t)}: \quad \rho_r c_r \frac{T_r^{(t+1)} - T_r^{(t)}}{\Delta t} =$$

$$= k_r \left[\frac{T_{r+1}^{(t)} + T_{r-1}^{(t)} - 2T_r^{(t)}}{\Delta r^2} + \frac{T_{r+1}^{(t)} - T_{r-1}^{(t)}}{2r\Delta r} \right] + q_{m,r}^{(t)} + \beta_r^{(t)} \cdot \left[T_{bla}^{(t)} - T_r^{(t)} \right]$$

and

$$\Omega_{Im} T_r^{(t)}: \quad \rho_r c_r \frac{T_r^{(t+1)} - T_r^{(t)}}{\Delta t} =$$

$$= k_r \left[\frac{T_{r+1}^{(t+1)} + T_{r-1}^{(t+1)} - 2T_r^{(t+1)}}{\Delta r^2} + \frac{T_{r+1}^{(t+1)} - T_{r-1}^{(t+1)}}{2r\Delta r} \right] + q_{m,r}^{(t+1)} + \beta_r^{(t+1)} \cdot \left[T_{bla}^{(t+1)} - T_r^{(t+1)} \right]$$

Here, the indices *r-1*, *r*, *r+1* refer to the preceding, the actual, and the next adjacent tissue node, respectively. Employing eq. (2) and separating the 'future' temperature terms the following numerical form of the bioheat equation is obtained:

$$[\gamma_r - 1]T_{r-1}^{(t+1)} + \left[\frac{\zeta_r}{\Delta t} + 2 + \delta_r \beta_r^{(t+1)} \right] T_r^{(t+1)} - [1+\gamma_r]T_{r+1}^{(t+1)} - \delta_r \beta_r^{(t+1)} T_{bla}^{(t+1)}$$

$$=$$

$$[1-\gamma_r]T_{r-1}^{(t)} + \left[\frac{\zeta_r}{\Delta t} - 2 - \delta_r \beta_r^{(t)} \right] T_r^{(t)} + [1+\gamma_r]T_{r+1}^{(t)} + \delta_r \left[q_{m,r}^{(t+1)} + q_{m,r}^{(t)} \right] + \delta_r \beta_r^{(t)} T_{bla}^{(t)}$$

$$(3)$$

where

$$\gamma_{r(cyl.)} = \frac{\Delta r}{2r} \qquad \gamma_{r(sph.)} = \frac{\Delta r}{r} \qquad \delta_r = \frac{\Delta r^2}{k_r} \qquad \zeta_r = 2\Delta r^2 \frac{\rho_r c_r}{k_r}.$$

The time step Δt [s] approximates the differential ∂t in eq. (1), and β_r [Wm^{-3}K^{-1}] denotes a time-dependent calorimetric equivalent of the nodal blood flow rate:

$$\beta_r = \rho_{bl} c_{bl} w_{bl,r}.$$

Equation (3) is applied to each of the 187 tissue nodes of the model using appropriate basal tissue material properties k, ρ, c, basal heat generation rates q_m, and basal blood perfusion rates w_{bl} (**Table 2**).

(**Table 2** about here)

The system of coupled linear equations is solved for each time and simulation iteration step using appropriate hybrid matrix solution techniques. For fast simulations the equation coefficients are organised as a structured system of time independent *conduction matrices* and time-dependent *blood matrices*. The coefficients of the *conduction matrices* include the constants γ_r, δ_r, ζ_r which describe the geometry and tissues' thermophysical properties, thus need to be computed only once in a simulation. They form the tri-diagonal conduction matrices with structure as shown in **Figure 2**.

(**Figure 2** about here)

Metabolic heat production

Metabolic heat generation within a tissue node volume is dealt with as a sum of the basal metabolic rate, $q_{m,bas,0}$ [W m^{-3}] and any additional heat gain, Δq_m [W m^{-3}]:

$$q_m = q_{m,bas,0} + \Delta q_m.$$

In thermal neutrality, no themoregulation occurs. In these conditions, the model's overall basal metabolism results in 87.1W which corresponds to the (standardized) whole-body metabolism of a reclining subject (ASHRAE Std.55, 2004). In muscles, the extra heat Δq_m contains three components: changes in the basal metabolic rate, $\Delta q_{m,bas}$, additional heat due to thermoregulatory shivering, $q_{m,sh}$, and exercise, $q_{m,w}$:

$$\Delta q_m = \Delta q_{m,bas} + q_{m,sh} + q_{m,w} \qquad (4)$$

Changes in the local basal metabolism, $\Delta q_{m,bas}$, refer to differences between the actual basal rate and basal rate in thermo-neutral conditions. This local autonomic regulation accounts for the

7

dependence of biochemical reaction on tissue temperature and is active in tissues where $q_{m,bas,0}$ is present and the local tissue temperature differs from its setpoint, T_0:

$$\Delta q_{m,bas} = q_{m,bas,0} \left[2^{(T-T_0)/10} - 1 \right]$$

The shivering term $q_{m,sh}$ [W m^{-3}] in eq. (4) is the local portion of the overall response elicited by the thermoregulatory system as described further below. The $q_{m,w}$-term [W m^{-3}] in eq. (4) can be written as:

$$q_{m,w} = \frac{c_{m,w} H}{V_{msc}}$$

where $c_{m,w}$ (**Table 4**) is a distribution coefficient (only for standing activities used in the UTCI-Fiala model), V_{msc} [m^3] the body-element muscle volume, and H [W] the internal whole body workload, i.e. that portion of the overall extra energy produced by muscular activity which does not appear as external work.

Blood circulation

The arterial blood temperature T_{bla} in eq. (3) arises from the actual overall thermal state of the body, and is obtained by simulating the human blood circulatory system. In addition to the original bioheat equation, also counter-current heat exchange between pairs of adjacent arteries and veins are simulated in the model.

The blood circulatory system model contains three main components: 1) central blood pool, 2) counter-current heat exchangers and 3) pathways to individual tissue nodes. In the circulation process body elements are supplied with blood from the central pool by major arteries. Before perfusing local tissues, arterial blood is regionally 'conditioned' by venous counter-current bloodstreams. Arterial blood then exchanges heat by convection in the capillary beds according to the bioheat equation before it is collected in major veins being re-warmed by heat from adjacent arteries as it flows back to the central blood pool. In the central blood pool, venous blood from all body parts is mixed to produce a 'new' central blood pool temperature.

The blood perfusion term in the bioheat equation is based on Fick´s first principle assuming that heat is exchanged solely in capillary beds. Counter-current heat exchange (CCX) is considered in the model to simulate the non-uniform distribution of arterial blood temperature (T_{bla}) over body parts. Assuming mass-continuity in blood vessels, any decrease of local arterial blood

temperature, T_{blp}-T_{bla}, due to CCX is equal to the increase of venous blood temperature, $T_{blv,X}$-T_{blv}, after undergoing CCX:

$$\sum_{r}^{nodes}\beta_r V_r\left(T_{blp}-T_{bla}\right) = \sum_{r}^{nodes}\beta_r V_r\left(T_{blv,X}-T_{blv}\right)$$

(5)

where T_{blp} is the central blood pool temperature, and T_{blv} and $T_{blv,X}$ are the element's venous temperatures before and after undergoing CCX, respectively. Since eq. (1) assumes that capillary blood reaches equilibrium with surrounding tissues, T_{blv} of a body element can be written as follows:

$$T_{blv} = \frac{\sum\limits_{r}^{nodes} T_r \beta_r V_r}{\sum\limits_{r}^{nodes}\beta_r V_r}.$$

(6)

Blood temperatures after undergoing CCX, i.e. T_{bla} and $T_{blv,X}$ are the two unknowns in eq. (5). In order to obtain element´s arterial blood temperature, T_{bla}, the net heat exchange between adjacent arteries and veins, Q_x, can be calculated as (Gordon et al, 1976):

$$Q_x = h_x\left(T_{bla}-T_{blv}\right)$$

(7)

where h_x is the corresponding counter-current heat exchange coefficient (**Table 2**). The arterial blood temperature, T_{bla}, of a body element is then obtained using eqs. (**Fehler! Verweisquelle konnte nicht gefunden werden. - Fehler! Verweisquelle konnte nicht gefunden werden.**) and rearranging:

$$T_{bla} = \frac{T_{blp}\sum\limits_{r}^{nodes}\beta_r V_r}{h_x + \sum\limits_{r}^{nodes}\beta_r V_r} + \frac{h_x\sum\limits_{r}^{nodes}T_r \beta_r V_r}{\sum\limits_{r}^{nodes}\beta_r V_r\left(h_x + \sum\limits_{r}^{nodes}\beta_r V_r\right)}$$

The equilibrium blood pool temperature, T_{blp}, is a function of *all* nodal tissue temperatures of the whole body underlining the 'coupling effect' of blood circulation in the human heat transfer:

9

$$T_{blp} = \cfrac{\sum_{i}^{elem.}\left(\cfrac{\sum_{r}^{nodes}\beta_{i,r}V_{i,r}}{h_{i,x}+\sum_{r}^{nodes}\beta_{i,r}V_{i,r}} \times \sum_{r}^{nodes}\beta_{i,r}V_{i,r}T_{i,r}\right)}{\sum_{i}^{elem.}\left[\cfrac{\left(\sum_{r}^{nodes}\beta_{i,r}V_{i,r}\right)^2}{h_{i,x}+\sum_{r}^{nodes}\beta_{i,r}V_{i,r}}\right]}$$

In thermal neutrality, tissues are supplied with arterial blood at basal rates β_0, i.e. basal perfusion rates, $w_{bl,0}$ (**Table 2**). In non-neutral conditions or during exercise, local blood perfusion rates vary with changes in regional metabolic rates, q_m. The increased demand for oxygen is accounted for using the gain factor $\Delta\beta$:

$$\Delta\beta = \mu_{bl}\ \Delta q_m$$

with a proportionality constant μ_{bl}=0.932 K^{-1} (Stolwijk, 1971). Using $\Delta\beta$, the actual local blood perfusion rate is obtained as:

$$\beta = \beta_0 + \Delta\beta.$$

The widely variable blood perfusion rates of the cutaneous plexus are subject to thermal regulation as described further below.

Nodal blood flow rates β are calculated for every time and iteration step of a simulation. They constitute the so called *blood matrices* which are superimposed with *conduction matrices* for each body element to solve the linear equation system for the whole body. A blood matrix of a body element is obtained by collecting the relevant terms of eq. (3) for all tissue nodes of that body element. For a (fictitious) four-node body element this yields:

$$\begin{pmatrix} \delta_1\beta_1 + B_x\beta_1^2 & B_x\delta_1\beta_2 & B_x\delta_1\beta_3 & B_x\delta_1\beta_4 \\ B_x\delta_2\beta_1 & \delta_2\beta_2 + B_x\beta_2^2 & B_x\delta_2\beta_3 & B_x\delta_2\beta_4 \\ B_x\delta_3\beta_1 & B_x\delta_3\beta_2 & \delta_3\beta_3 + B_x\beta_3^2 & B_x\delta_3\beta_4 \\ B_x\delta_4\beta_1 & B_x\delta_4\beta_2 & B_x\delta_4\beta_3 & \delta_4\beta_4 + B_x\beta_4^2 \end{pmatrix}$$

where

$$B_x = \frac{-h_x \delta_r V_r}{\sum\limits_{r}^{nodes} \beta_r V_r \left(h_x + \sum\limits_{r}^{nodes} \beta_r V_r \right)}$$

The superimposed conduction and blood sub-matrices of individual body elements form the *whole body coefficient matrix*. The structure of this matrix to be solved for each simulation iteration step is plotted in **Figure 3**.

(**Figure 3** about here)

Solving the whole body matrix for the undressed, reclining model person exposed to steady state thermo-neutral conditions of 30°C, results in a mean skin temperature of 34.3 °C and body core temperatures of 37.0 °C in the head core (hypothalamus) and 36.9 °C in the abdomen core (rectum).

Heat exchange with the environment

The largest portion of bodily heat is typically released to the environment from the body surface but some heat is also lost by respiration. For each sector of the body surface, heat and mass balances are established to calculate local net heat exchanges with the environment. The convective heat exchange q_{cnv} [W m^{-2}] between a body sector of surface temperature T_{bs} and ambient air of temperature T_a is calculated by considering both natural and forced convection using combined-convection coefficients, $h_{c,mix}$:

$$q_{cnv} = h_{c,mix} \left(T_{bs} - T_a \right)$$

The convection coefficients, $h_{c,mix}$ [W m^{-2}K^{-1}], are calculated as a function of the location at the body, the temperature difference between the sector surface and the air, and the local air speed v_a [m/s]:

$$h_{c,mix} = \sqrt{ a_{nat} \sqrt{T_{bs} - T_a} + a_{for} \cdot v_a + a_{mix} }$$
(8)

The $h_{c,mix}$ equations (**Table 3**) were derived from measurements of local heat losses from a heated full-scale manikin with realistic skin temperature distributions for both natural and forced convection conditions (Wang 1990). The local air velocity, v_a [m/s], is calculated in the model (used for developing UTCI) from meteorological wind speed measurement at 10 m height above ground, v_{Zr} (Oke 1987):

$$v_a = v_{Zr} \frac{\log(Z/z0)}{\log(Zr/z0)}$$

where Z [m] is the height of the body element (centre) above ground, Zr [m] is the reference height of the meteorological measurement, i.e., 10 m, and $z0$ [m] is the roughness length, assumed to be 0.01 m for purposes of UTCI.

(**Table 3** about here)

To calculate the long wave portion of the radiative heat exchange (q_{rlw}), the model employs the concept of (directional) mean surface temperatures of the radiant envelope that encloses a body sector using the corresponding sector's view factor:

$$q_{rlw} = \sigma\, \varepsilon_{bs}\, \varepsilon_{env}\, \phi_{bs-env} \left[(T_{bs} + 273)^4 - (T_{env} + 273)^4 \right]$$

where $\sigma = 5.67 \times 10^{-8}$ W m^{-2} K^{-4} is the Stefan-Bolzmann constant, ε_{bs} and ε_{env} are the surface emissivity of the body sector (**Table 3**, ε_{bs}=0.95 for UTCI clothing) and the radiant envelope (ε_{env} =1.0 for UTCI envelopes), respectively. The view factors ϕ_{bs-env} (**Table 3**) of the curved body sector surfaces with respect to the enclosure 'seen' are based on numerical radiation simulations using detailed 3D human geometry models (Kubaha et al, 2004). T_{bs} and T_{env} [°C] are the surface temperatures of the body sector and the envelope, respectively.

In the UTCI-Fiala model, any short wave radiation q_{rsw} [W m^{-2}] absorbed by a sector surface is calculated as:

$$q_{rsw} = \alpha_{bs} \, f_s \, I_s$$

where α_{bs} is the short-wave absorptivity of the body surface which depends on the colour of skin or the material covering the sector, I_s [Wm^{-2}] is the incident short-wave radiation, and f_s the corresponding body sector's projected area factor (for unknown body orientation) which depends on body posture and the solar altitude. It should however be noted that in UTCI solar radiation is not treated explicitly but is part of the process for calculating the environmental mean radiant temperature.

The incorporated skin evaporation model ensures heat and mass balances at each body sector surface. The latent energy transport from a skin sector of area A_{sk} is given by (Fiala et al. 1999):

$$\frac{p_{sk} - p_a}{R_{e,cl,l}} = \lambda_{H_2O} \frac{dm_{sw}}{A_{sk} \, dt} + \frac{p_{osk,sat} - p_{sk}}{R_{e,osk}} \tag{9}$$

The left-hand side of the equation represents the net energy transport due to the evaporative potential between skin and air, where p_{sk} and p_a [Pa] are the partial water vapour pressure at the skin surface and of the ambient air, respectively, and $R_{e,cl,l}$ is the local evaporative resistance of any (multi-layered) clothing covering that body sector.

The first right-hand term of eq. (9) accounts for evaporation of sweating from the skin, where λ_{H_2O} is the heat of vaporisation of water and dm_{sw}/dt the local rate of regulatory sweating. The last term of eq. (9) describes heat transport by moisture diffusion through the skin with $p_{osk,sat}$ as the saturated partial vapour pressure within the outer skin (Jones and Ogawa, 1992). The model uses a moisture permeability of the outer skin of $1/R_{e,sk}$=0.003 W m^{-2}Pa^{-1} (ISO 7730, 2005) which produces a basal skin wettedness of wt_{sk}=0.06 in thermo-neutral conditions.

The net evaporative heat loss of a skin sector depends on the actual local vapour pressure p_{sk} [Pa] found at the sector's skin surface. This quantity is calculated by re-arranging eq. (9):

$$p_{sk} = \frac{\lambda_{H_2O} \dfrac{dm_{sw}}{A_{sk} \, dt} + \dfrac{p_{osk,sat} - p_{sk}}{R_{e,osk}} + \dfrac{p_a}{R_{e,cl,l}}}{1\big/R_{e,cl,l} + 1\big/R_{e,osk}}$$

The evaporation model accounts for storage of sweat liquid at the skin surface as described by Jones and Ogawa (1992). Moisture of up 35 g m^{-2} can be accumulated when p_{sk} exceeds its

saturation level, $p_{sk,sat}$ [Pa], but quantities exceeding this threshold would run off. The rate of moisture storage dm_{acc}/dt [kg/s] is then equivalent to the rate of moisture production dm_{sw}/dt less the rate of moisture evaporation:

$$\frac{dm_{acc}}{A_{sk}dt} = \frac{dm_{sw}}{A_{sk}dt} - \frac{p_{sk,sat} - p_a}{R_{e,cl,l} \, \lambda_{H_2O}}$$

The incorporated clothing model is based on modelling heat and mass transfer within multi-layer cloth composites according to McCullough et al. (1985, 1989) accounting for local thermal and evaporative resistances, R_{cl} [m²K/W] and $R_{e,cl}$ [m²Pa/W], respectively, of each body element. That clothing model was extended in the *UTCI-Fiala* model for effects relevant to human exposure to outdoor climates as described by Havenith et al. (2011) in this special issue. The incorporated respiratory heat exchange model is obtained from the work of Fanger (1973) taking into account both heat losses by evaporation and convection. The latent heat exchange is calculated according to Fanger from the pulmonary ventilation rate which is a function of the whole body metabolism, $\int q_m dV$, latent heat of vaporisation of water, and the difference between humidity ratio of the expired and inspired air which depends on the air temperature, T_a [°C], and the partial vapour pressure of the ambient air, p_a [Pa]:

$$E_{rsp} = 3.233 \cdot \int q_m \, dV \left(0.0277 - 6.5 \times 10^{-5} T_a - 4.91 \times 10^{-6} \times p_a \right)$$

Since the enthalpy of the expired air depends to a certain degree upon the condition of the inspired air, E_{rsp} appears as a function of both T_a and p_a. The inclusion of T_a (neglected by Fanger for moderate conditions) allows E_{rsp} to be calculated adequately for a wide range of ambient air conditions.

The dry heat loss of respiration due to the temperature difference between expired and inspired air, is according to Fanger (1973) described as a function of the pulmonary ventilation rate, and the temperature and vapour pressure of the ambient air, T_a and p_a, respectively:

$$C_{rsp} = 1.44 \times 10^{-3} \times \int q_m \, dV \left(32.6 - 0.934 \times T_a + 1.96 \times 10^{-4} \times p_a \right)$$

The total respiratory heat loss $E_{rsp} + C_{rsp}$ is distributed over body elements of the pulmonary tract: face, neck and lung.

14

Thermoregulatory system and perceptual responses

The model predicts the four essential thermoregulatory responses of the central nervous system, i.e. suppression (vasoconstriction), elevation (dilatation) of the cutaneous blood flow, shivering, and sweat moisture excretion (Fiala et al. 2001). The thermoregulatory system was developed by means of regression analysis using measured data obtained from physiological experiments covering steady state and transient cold stress, cold, moderate, warm and hot stress conditions, and activity levels of up to heavy exercise. Statistical regression analysis was employed to determine (i) the input signals which are involved in regulatory processes (only statistically significant signals are used) and (ii) quantitative control equation relationships for the individual responses. A block diagram of the Fiala regulatory system model is shown in **Figure 4**.

(**Figure 4** about here)

The system coefficients of the thermoregulatory system are a result of meta-regression analysis (Fiala et al, 2001) and are non-linear functions of the respective punitive signals, **Figure 5**.

(**Figure 5** about here)

The following control equations govern the individual thermoregulatory responses in the model:

$$SH = 10 \left[tanh \left(0.48\,\Delta T_{sk,m} + 3.62 \right) - 1 \right] \Delta T_{sk,m} - 27.9\,\Delta T_{hy} + 1.7\,\Delta T_{sk,m} \frac{dT_{\bar{sk,m}}}{dt} - 28.6$$

$$CS = 35 \left[tanh \left(0.34\,\Delta T_{sk,m} + 1.07 \right) - 1 \right] \Delta T_{sk,m} + 3.9\,\Delta T_{sk,m} \frac{dT_{\bar{sk,m}}}{dt}$$

$$DL = 21 \left[tanh \left(0.79\,\Delta T_{sk,m} - 0.70 \right) + 1 \right] \Delta T_{sk,m} + 32 \left[tanh \left(3.29\,\Delta T_{hy} - 1.46 \right) + 1 \right] \Delta T_{hy}$$

$$SW = \left[0.8\,tanh \left(0.59\,\Delta T_{sk,m} - 0.19 \right) + 1.2 \right] \Delta T_{sk,m} + \left[5.7\,tanh \left(1.98\,\Delta T_{hy} - 1.03 \right) + 6.3 \right] \Delta T_{hy}$$

where SH [W], CS [ ], DL [W/K], and SW [g/min] are the overall effectors of the central nervous system, i.e. shivering, peripheral vasoconstriction and dilatation, and sweating, respectively. In

15

the model, SH has a theoretical maximum of 350W but is compensated by the amount of any extra heat generated due to exercise in the UTCI-Fiala model. The CS and SW responses have a maximum value of 600 W/K and 23 g/min, respectively. $\Delta T_{sk,m}$ and ΔT_{hy} are afferent signals associated with the sensitivity-weighted mean skin temperature and the hypothalamus temperature, respectively. The skin area and sensitivity coefficients used to calculate the mean skin temperature are listed in **Table 4**. The $dT_{sk,m}/dt$ term represents negative rates of change of the mean skin temperature as a dynamic signal influencing regulatory responses against cold, i.e. *SH* and *CS*. The overall responses *SH, CS, DL*, and *SW* are distributed over the body using distribution coefficients listed in **Table 4**. The distribution coefficients for sweating and vasodilation were obtained from Stolwijk (1971). The coefficients used in the UTCI-Fiala model to distribute the overall shivering and vasoconstriction responses were estimated from simulations of cold and extreme-cold exposures (Fiala et al. 2001), while the skin sensitivity coefficients were obtained from Nadel et al. (1973) and Crawshaw et al. (1975).

(**Table 4** about here)

The model predicts local skin blood perfusion rates, β_i [W/K], based on a relationship which recognises that i) the flow rate is reduced or elevated via separate regulatory mechanisms of peripheral vasoconstriction (*CS*) and vasodilatation (*DL*) (Rowell and Wyss 1985), and ii) the local perfusion rate can be about doubled by a 10K-increase in local skin temperature (Stolwijk 1971):

$$\beta_i = \frac{\beta_{0,i} + a_{dl,i}\, DL}{1 + a_{cs,i}\, CS \cdot e^{-DL/80}} \times 2^{\frac{T_{sk,i} - T_{sk,i,0}}{10}}$$

where $\beta_{0,i}$ arises from the basal skin blood flow $SBF_{0,i}$: $\beta_{0,i} = \rho_{bl}\, c_{bl}\, SBF_{0,i}$; $a_{dl,i}$ and $a_{cs,i}$ are distribution coefficients (**Table 4**); $T_{sk,i}$ and $T_{sk,i,0}$ are the actual and the reference surface temperature of the i-*th* skin sector. DL and CS represent the overall peripheral vasomotor responses described above.

The local sweat rate, $dm_{sw,i}/dt$ [g/min], is predicted by weighting the central nervous system effector signal, SW [g/min], by local influences, i.e. the local skin temperature (Nadel et al. 1971):

$$\frac{dm_{sw,i}}{dt} = a_{sw,i}\, SW \times 2^{\frac{T_{sk,i} - T_{sk,i,0}}{10}}$$

where $a_{sw,i}$ is the fraction of the total sweating stimulus at the i-th skin sector (**Table 4**), $T_{sk,i}$ and $T_{sk,i,0}$ are the predicted skin temperature of each sector and the corresponding reference value, respectively.

The model predicts perceptual responses from physiological body states (Fiala et al, 2003). Comfort experiments involving over 2000 male and female subjects, and covering a wide range of steady state and transient environmental temperatures, relative humidities, and activity levels served as a basis for developing the Dynamic Thermal Sensation, DTS using the seven-point ASHRAE scale (ASHRAE Std.55, 2004) running from -3 for cold to +3 for hot. The comfort model was developed by correlating series of experimentally observed overall thermal sensation votes with dynamically predicted variables of the bodily thermal states.

Regression analysis revealed temperature signals from the skin, the head core, and rates of change of the skin temperature to be the driving impulses which govern the human overall Thermal Sensation. The model for predicting Dynamic Thermal Sensation, DTS, has the form (Fiala et al, 2003):

$$ DTS = 3 \times \tanh \left(a \, \Delta T_{sk,m} + g + \frac{0.11 \frac{dT_{sk,m}}{dt}^{(-)} + 1.91 e^{-0.68 \, lt} \times \frac{dT_{sk,m}}{dt}^{(+)}_{max}}{1+g} \right) $$

where a is 0.30 K^{-1} and 1.08 K^{-1} for $\Delta T_{sk,m} < 0$ and $\Delta T_{sk,m} > 0$, respectively; $dT_{sk,m}^{(-)}/dt = 0$ for $dT_{sk,m}/dt > 0$, $dT_{sk,m}^{+}/dt_{max}$ the maximum positive rate of change of skin temperature with t the time elapsed since the occurrence of $dT_{sk,m}^{+}/dt_{max}$, and g is calculated by:

$$ g = 7.94 \times \exp \left(\frac{-0.902}{\Delta T_{hy} + 0.4} + \frac{7.612}{\Delta T_{sk,m} - 4} \right) $$

Discussion

The Fiala model has been subject to general as well as application-specific validation studies regarding human thermal and regulatory behaviours (e.g. Fiala et al. 2001), occupant comfort in buildings (Fiala et al. 2003), transient indoor climate conditions in cars (Fiala et al. 2004), asymmetric radiation scenarios and exposures to high intensity sources (Kubaha 2005, Richards

and Fiala 2004), but also anaesthesia and clinical trials. A summary is provided in Fiala et al. (2010).

Generally, the various validation studies revealed consistent predictions in line with experimental observations with respect to thermoregulatory and thermal sensation responses, mean and local skin temperatures and internal temperatures for the analysed range of environmental temperatures between 5 °C and 50 °C and activity levels between 0.8 and 9 met. Mean and local skin temperatures agreed with experimental observations typically within ±1 K, body core temperatures within ±0.3 K, shivering and sweating responses within 30 W, and perceptual responses within ±1 scale units of the 7-point ASHRAE scale.

A large-scale validation study has been conducted as part of COST Action 730. This work, described by Psikuta et al. (2011) in this special issue, is concerned with comparisons of model predictions with measured data obtained from climate chamber or wind tunnel experiments as well as field surveys conducted outdoors. Other COST Action 730 validation tests of the UTCI-Fiala model are described in Bröde et al. (2011b) and Kampmann et al. (2010) in this special issue.

Following the successful validation tests, the UTCI-Fiala model was used to derive the UTC Index which employs the concept of equivalent human physiological responses to combinations of air temperature, radiation, wind and humidity, as described by Bröde et al. (2011a) in this special issue. The flexibility of the model makes future extensions and further development of the UTCI concept possible including, for example, considering different levels of activity, different clothing habits or protective clothing for special purpose applications, and the definition of climate indices for different world regions. Although the model version described in this paper does not account for effects such as the impact of physical fitness, state of acclimatisation, age or gender on thermoregulatory responses, these features shall be implemented through future developments.

Acknowledgements

References

Aschoff VJ, Wever R (1958) Kern und Schale im Wärmehaushalt des Menschen. Naturwissenschaften 45: 477-485

ASHRAE (2004) ANSI/ASHRAE Standard 55: Thermal Environmental Conditions for Human Occupancy, Atlanta, GA, American Society of Heating, Refrigeration and Air-Conditioning Engineers, Inc

Azer NZ, Hsu S (1977) The prediction of thermal sensation from a simple model of human physiological regulatory response. ASHRAE Trans 83(I): 88-102

Burton AC (1937) The application of the theory of heat flow to the study of energy metabolism. J Nutrition: 487-533

Bröde P, Fiala D, Blazejczyk K, Holmér I, Jendritzky G, Kampmann B, Tinz B, Havenith G (2011a) Deriving the Operational Procedure for the Universal Thermal Climate Index UTCI. Int J Biometeorol ??: ??-??

Bröde P, Krüger EL, Rossi FA, Fiala D (2011b) Predicting urban outdoor thermal comfort by the universal thermal climate index UTCI – A case study in southern Brazil. Int J Biometeorol ??: ??-??

Crawshaw LI, Nadel ER, Stolwijk JAJ, Stamford BA (1975) Effect of local cooling on sweating rate and cold sensation. Pflügers Arch 354: 19-27

Fanger P.O. (1973) Thermal Comfort - Analysis and Applications in Environmental Engineering. McGraw-Hill, New York - London - Sidney – Toronto

Fiala D (1998) Dynamic simulation of human heat transfer and thermal comfort. PhD Thesis, De Montfort University, UK

Fiala D, Lomas KJ, Stohrer M (1999) A computer model of human thermoregulation for a wide range of environmental conditions: The passive system. J Appl Physiol 87: 1957-1972

Fiala D, Lomas KJ, Stohrer M (2001) Computer prediction of human thermoregulatory and temperature responses to a wide range of environmental conditions. Int J Biometeorol 45: 143-159

Fiala D, Lomas KJ, Stohrer M (2003) First Principles Modelling of Thermal Sensation Responses in Steady State and Transient Boundary Conditions. ASHRAE Trans 109 (1): 179-186

Fiala D, Bunzl A, Lomas KJ, Cropper PC, Schlenz D (2004) A New Simulation System for Predicting Human Thermal and Perceptual Responses in Vehicles. In: D. Schlenz (ed). PKW-Klimatisierung III: Klimakonzepte, Regelungsstrategien und Entwicklungsmethoden. Expert Verlag Renningen, Haus der Technik Fachbuch Band 27: 147-162

Fiala D, Psikuta A, Jendritzky G, Paulke S, Nelson DA, van Marken Lichtenbelt WD, Frijns AJH (2010) Physiological modeling for technical, clinical and research applications. Front Biosci S2: 939-968

Gagge AP, Fobelets AP, Berglund PE (1986) A standard predictive index of human response to the thermal environment. ASHRAE Trans 92: 709-731

Gordon RG, Roemer RB, Horvath SM (1976) A mathematical model of the human temperature regulatory system - transient cold exposure response. IEEE Trans Biomed Eng 23: 434-444

Havenith G, Fiala D, Blazejczyk K, Richards M, Bröde P, Holmér I, Rintamäki H, Benshabat Y, Jendritzky G (2011) The UTCI-Clothing Model. Int J Biometeorol ??: ??-??

Huizenga C, Zhang H, Arens E (2001) A model of human physiology and comfort for assessing complex thermal environments. Build Environ 36(6): 691-699

ISO 7730 (2005) Ergonomics of the thermal environment - Analytical determination and interpretation of thermal comfort using calculation of the PMV and PPD indices and local thermal comfort criteria. International Organisation for Standardisation, Geneve

Jones BW, Ogawa Y (1992) Transient interaction between the human and the thermal environment. ASHRAE Trans. 98: 189-196

Kampmann B, Bröde P, Fiala D (2011) Physiological responses to temperature and humidity compared to the assessment by UTCI, WGBT and PHS. Int J Biometeorol ??: ??-??

Kubaha K, Fiala D, Toftum J, Taki AH (2004) Human projected area factors for detailed direct and diffuse solar radiation analysis. Int J Biometeorol 49: 113-129

Kubaha K (2005) Asymmetric radiation and human thermal comfort: PhD Thesis, De Montfort University, UK

McCullough EA, Jones BW, Huck J (1985) A comprehensive data base for estimating clothing insulation. ASHRAE Trans 92: 29-47

McCullough EA, Jones BW, Tamura T (1989) A data base for determining the evaporative resistance of clothing. ASHRAE Trans 95: 316-328

Nadel ER, Bullard RW, Stolwijk JAJ (1971) Importance of skin temperature in the regulation of sweating. J Appl Physiol 31: 80-87

Nadel ER, Mitchell JW, and Stolwijk JAJ (1973) Differential thermal sensitivity in the human skin. Pflügers Arch 340: 71-76

Oke TR (1987) Boundary Layer Climates, Routledge, London, pp. 453

Pennes HH (1948) Analysis of tissue and arterial blood temperatures in the resting human forearm. J Appl Physiol 1: 93-122

Psikuta A Fiala D, Laschewski G, Jendritzky G, Richards M, Blazejczyk K, Mekjavic I, Rintamäki H, Havenith G, de Dear R (2011) Evaluation of the Fiala multi-node thermophysiological model for UTCI application. Int J Biometeorol ??: ??-??

Richards M, Fiala D (2004) Modelling fire-fighter responses to exercise and asymmetric IR-radiation using a dynamic multi-mode model of human physiology and results from the Sweating Agile thermal Manikin (SAM). Eur J Appl Physiol 92(6): 649-653

Stolwijk JAJ (1971) A mathematical model of physiological temperature regulation in man. NASA contractor report, NASA CR-1855, Washington DC.

Tanabe S, Kobayashi K, Nakano J, Ozeki Y, Konishi M (2002) Evaluation of thermal comfort using combined multi-node thermoregulation (65MN) and radiation models and computational fluid dynamics (CFD). Energ Buildings 34(6): 637-646

Wang X-L (1990) Convective heat losses from segments of the human body. Climate and Buildings 3: 8-14

Weinbaum S, Jiji LM, Lemons DE (1984) Theory and experiment for the effect of vascular microstructure on surface tissue heat transfer - part I: anatomical foundation and model conceptualization. ASME J. Biomech. Eng. 106: 321-330

Wissler EH (1985) Mathematical simulation of human thermal behavior using whole body models. In: A. Shitzer, R.C. Eberhart (eds): Heat transfer in medicine and biology – analysis and applications, Plenum New York London: 325–373

Tables

Table 1: Body geometry parameters

Body element	Length	Outer radius	Central angle	Surface area	Spatial Sectors - angle [deg]			
	[m]	[m]	[deg]	[m²]	anterior	posterion	inferior	superior
head		0.1040	180.0	0.068	16.0	164.0		
face	0.0984	0.0780	210.0	0.028	98.0			112.0
neck	0.0842	0.0567	360.0	0.030	58.0	80.0		222.0
shoulders	0.3200	0.0460	130.0	0.033				130.0
thorax	0.3060	0.1290	360.0	0.248	165.0	149.0	46.0	
abdomen	0.5520	0.1260	360.0	0.230	133.0	131.0	96.0	
upper arms	0.6380	0.0430	360.0	0.172	77.0	76.0	52.0	155.0
lower arms	0.6360	0.0404	360.0	0.161	44.0	59.0	128.0	129.0
hands	0.6200	0.0226	360.0	0.088			183.0	177.0
upper legs	0.7020	0.0584	360.0	0.258	95.0	79.0	83.0	103.0
lower legs	0.6880	0.0511	360.0	0.221	68.0	99.0	89.0	104.0
feet	0.4800	0.0350	360.0	0.106	239.0	121.0		

Table 2: *Thermophysical and -physiological parameters*.

Body element	Counter-current heat exch. coeff. h_x $W\,K^{-1}$	Tissue material	Conductivity k $W\,m^{-1}K^{-1}$	Density ς $kg\,m^{-3}$	Heat capacitance c $J\,kg^{-1}K^{-1}$	Blood perfusion rate $w_{bl,0}$ $L\,s^{-1}m^{-3}$	Basal metabolism rate $q_{m,0}$ $W\,m^{-3}$
head	0.000	brain	0.49	1080	3850	10.132	13400
		bone	1.16	1500	3850	0	0
		fat	0.16	850	2300	0.0036	58
		skin	0.47	1085	3680	5.48	368
face	0.000	muscle	0.42	1085	3768	0.538	684
		bone	1.16	1500	3850	0	0
		muscle	0.42	1085	3768	0.54	684
		fat	0.16	850	2300	0	58
		skin	0.47	1085	3680	11.17	368
neck	0.000	bone	0.75	1357	1700	0	0
		muscle	0.42	1085	3768	0.538	684
		fat	0.16	850	2300	0.0036	58
		skin	0.47	1085	3680	6.8	368
shoulders	0.000	bone	0.75	1357	1700	0	0
		muscle	0.42	1085	3768	0.538	684
		fat	0.16	850	2300	0.0036	58
		skin	0.47	1085	3680	1.01	368
thorax	0.000	lung	0.28	550	3718	CO	600
		bone	0.75	1357	1700	0	0
		muscle	0.42	1085	3768	0.538	684
		fat	0.16	850	2300	0.0036	58
		skin	0.47	1085	3680	1.58	368
abdomen	0.000	core	0.53	1000	3697	4.31	4100
		bone	0.75	1357	1700	0	0
		muscle	0.42	1085	3768	0.538	684
		fat	0.16	850	2300	0.0036	58
		skin	0.47	1085	3680	1.44	368
upper arms	2.065	bone	0.75	1357	1700	0	0
		muscle	0.42	1085	3768	0.538	684
		fat	0.16	850	2300	0.0036	58
		skin	0.47	1085	3680	1.1	368
lower arms	6.195	bone	0.75	1357	1700	0	0
		muscle	0.42	1085	3768	0.538	684
		fat	0.16	850	2300	0.0036	58
		skin	0.47	1085	3680	1.1	368
hands	0.570	bone	0.75	1357	1700	0	0
		muscle	0.42	1085	3768	0.538	684
		fat	0.16	850	2300	0.0036	58
		skin	0.47	1085	3680	4.54	368
upper legs	3.450	bone	0.75	1357	1700	0	0
		muscle	0.42	1085	3768	0.538	684
		fat	0.16	850	2300	0.0036	58
		skin	0.47	1085	3680	1.05	368
lower legs	9.350	bone	0.75	1357	1700	0	0
		muscle	0.42	1085	3768	0.538	684
		fat	0.16	850	2300	0.0036	58
		skin	0.47	1085	3680	1.05	368
feet	1.450	bone	0.75	1357	1700	0	0
		muscle	0.42	1085	3768	0.538	684
		fat	0.16	850	2300	0.0036	58
		skin	0.47	1085	3680	1.1	368

Table 3*: Environmental heat exchange parameters.*

Body element	Mixed convection heat transfer coefficient $h_{c,mix}$			Surface absorptivity α_{bs}	View factors (standing posture) between body sector and the environment ϕ_{bs-env}			
	[W/(m²K)]			[ ]	[ ]			
	a_{nat}	a_{for}	a_{mix}		anterior	posterior	inferior	superior
head	3.000	113.00	-5.650	0.80	0.9869	0.9643		
face	3.000	113.00	-5.650	0.99	0.8417	0.8909		
neck	1.600	130.00	-6.500	0.99	0.7792	0.9433	0.8569	
shoulders	5.900	216.00	-10.800	0.99	0.9048			
thorax	0.500	180.00	-7.400	0.99	0.9314	0.9590	0.4408	
abdomen	1.200	180.00	-9.000	0.99	0.8923	0.8886	0.6323	
upper arms	8.270	216.02	-10.801	0.99	0.7546	0.9268	0.3356	0.9821
lower arms	8.270	216.02	-10.801	0.99	0.8774	0.9639	0.5065	0.9967
hands	8.270	216.02	-10.801	0.99	0.8835	0.3801		
upper legs	5.300	220.00	-11.000	0.99	0.8761	0.9374	0.4693	0.8793
lower legs	5.300	220.00	-11.000	0.99	0.9282	0.9393	0.7264	0.9800
feet	6.800	210.00	-10.500	0.99	0.8602	0.8955		

**Table 4**: *Skin sensitivity, workload and regulatory response distribution coefficients.*

	Skin sensitivity*	Work load (standing activities)	Thermoregulatory system			
			sweating	dilatation	constriction	shivering
Body element	a_{sk}	c_w	a_{sw}	a_{dl}	a_{cs}	a_{sh}
head	0.0835	0.0000	0.0570	0.0550	0.0040	0.0000
face	0.0418	0.0000	0.0240	0.0460	0.0313	0.0020
neck	0.0417	0.0120	0.0270	0.0310	0.0140	0.0020
shoulders	0.0300	0.0220	0.0300	0.0200	0.0150	0.0002
thorax	0.1290	0.0700	0.2200	0.1410	0.0002	0.6305
abdomen	0.1210	0.1910	0.2030	0.1610	0.0205	0.2400
upper arms	0.0900	0.0480	0.0800	0.0410	0.1020	0.0240
lower arms	0.0900	0.0320	0.0750	0.0540	0.1345	0.0160
hands	0.0900	0.0150	0.0310	0.1210	0.1150	0.0020
upper legs	0.1040	0.4000	0.1170	0.0950	0.1360	0.0520
lower legs	0.1040	0.1600	0.1010	0.1340	0.2425	0.0293
feet	0.0750	0.0500	0.0350	0.1010	0.1850	0.0020

* used to calculate mean skin temperature

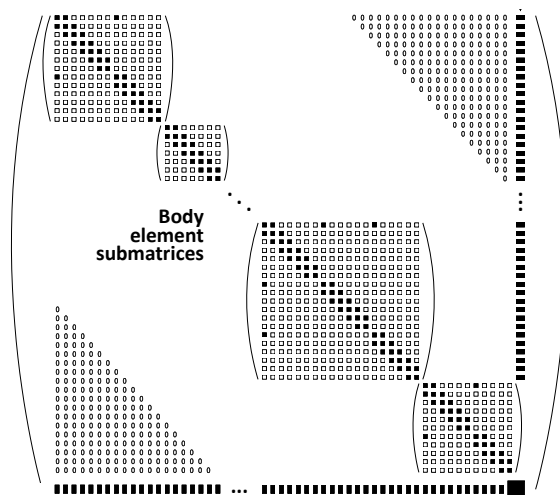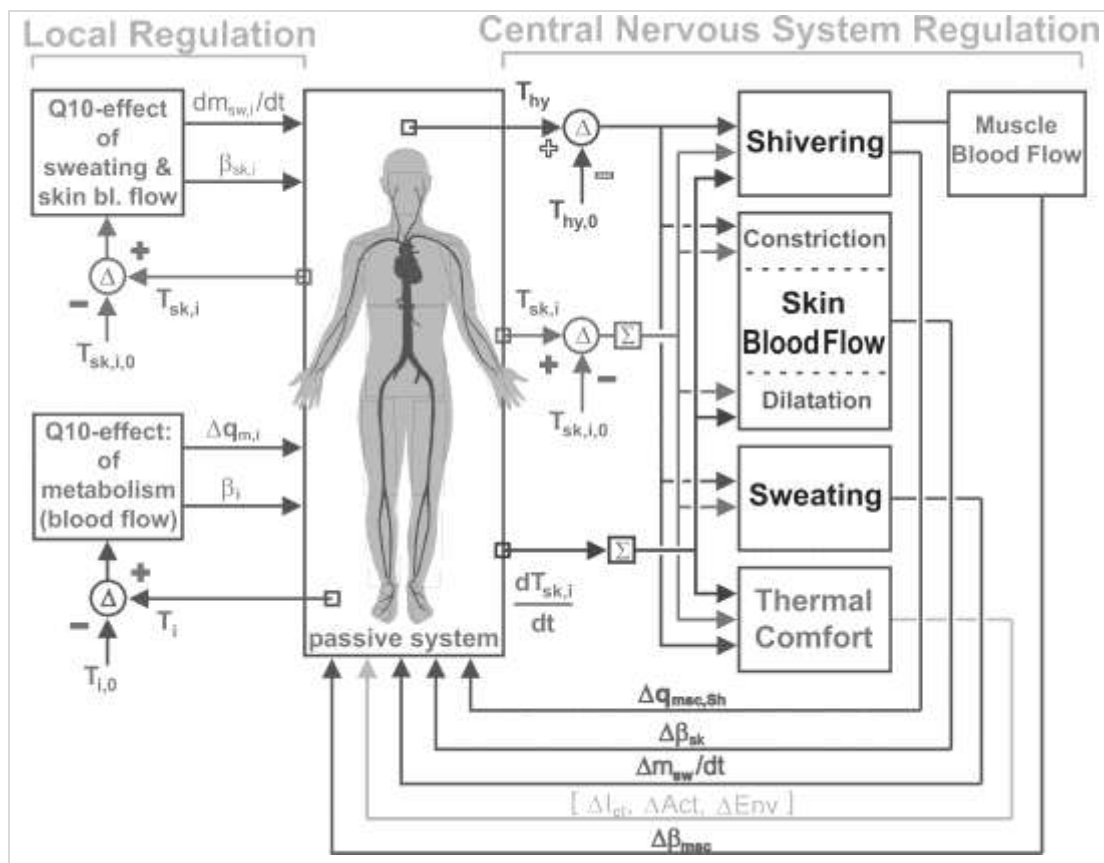# Figures
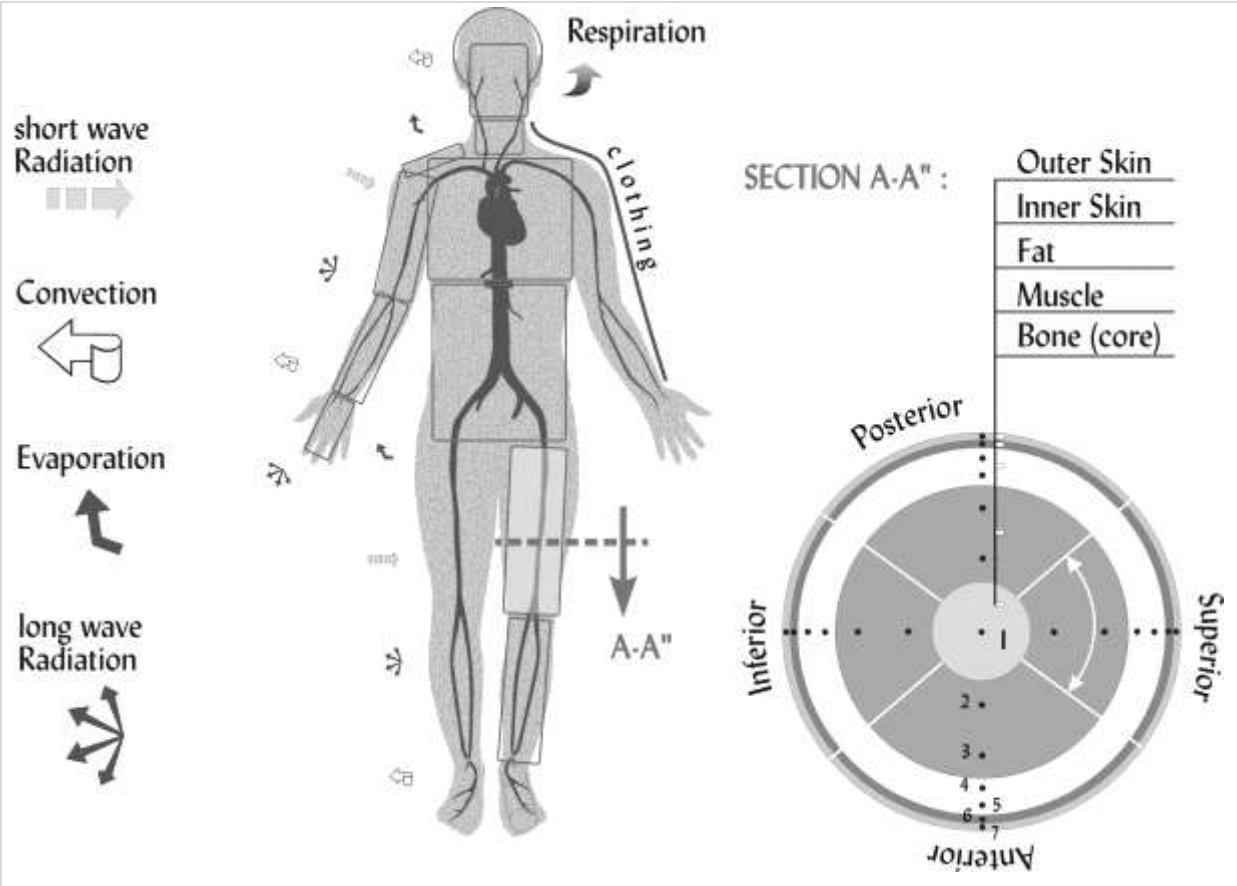
Figure 1: Schematic diagram of the UTCI-Fiala model.
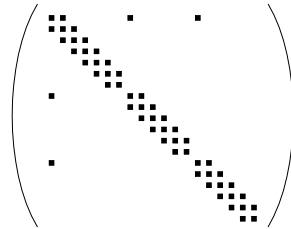
Figure 2: Tri-diagonal structure of non-zero coefficients of an element's 'conduction' matrix (redrawn from Fiala et al. 1999, http://jap.physiology.org/content/87/5/1957.abstract).

Figure 3: Structure of the resultant whole body matrix (redrawn from Fiala et al. 1999).

Figure 4: *Block diagram of the Fiala thermoregulatory system model (redrawn from Fiala et al. 2001, 2010). The central nervous system thermoregulation (CNS) accounts for overall changes in muscle metabolism by shivering (and the corresponding changes in muscle blood flow), skin blood flow by vasodilatation and vasoconstriction, and skin moisture extretion by sweating. The model uses temperatures of the skin (T_{sk}) and of the head core (hypothalamus, T_{hy}) as well as the rate of change of skin temperature ($dT_{sk,i}/dt$) as input signals into the regulatory centre. The local autonomic regulation employs local skin and tissue temperatures, $T_{sk,i}$ and T_i, to modify local sweat rates, local blood flows, and tissue metabolic rates.*

Figure 5: *Control equation coefficients as non-linear functions of temperature signals from the body core and body periphery (with kind permission from Springer Science+Business Media: Fiala et al. 2001, Figs. 3,5-9).*